

Influence of hemp protein hydrolysates on the textural, thermal, rheological, and structural properties of corn starch with varying amylose content

Gaosheng Wu, Lokesh Kumar ^{*} , James D. Morton, Hannah Lee ^{*}

Department of Wine, Food and Molecular Biosciences, Faculty of Agriculture and Life sciences, Lincoln University, Lincoln 7647, New Zealand

ARTICLE INFO

Keywords:

Hemp protein hydrolysates
Amylose content
Thermal properties
Texture properties
Particle size distribution
Rheological properties
Fourier transform infrared spectroscopy (FT-IR)

ABSTRACT

Over the past decades, researchers have investigated the changes in physical, chemical, and nutritional properties of starch blended with various biomolecules. Hemp seed meal is a sustainable byproduct of hempseed oil extraction, and there is limited research on the use of hemp protein hydrolysates, prepared from this hemp seed meal, as a food ingredient. This study investigated the physicochemical properties of hemp protein hydrolysates (HPH) and corn starch complexes using corn starch with varying amylose contents: waxy corn starch (WCS, 1% amylose), normal corn starch (NCS, 27% amylose) and high-amylose corn starch (HACS, 68% amylose). The addition of the HPH to the starch significantly modified the textural properties of starch gels, particularly enhancing elasticity and hardness in WCS and NCS, and increasing adhesiveness in NCS and HACS. Notable effects were observed with 20% HPH (HPH hydrolyzed by pepsin) on WCS elasticity, 10% HPHB (HPH hydrolyzed by bacterial protease) on WCS hardness, and 20% HPHB on WCS adhesiveness. Particle size distribution indicated substantial granule size increases, especially in HACS. FT-IR analysis revealed shifts in absorption peaks, suggesting altered hydrogen bonding interactions without new functional groups. The addition of protein hydrolysates further amplified the thermal properties of starch, particularly in HACS. Rheological properties varied, with increased storage (G') and loss (G'') moduli in NCS-HPH mixtures and general decreases in WCS-HPH and HACS-HPH. The findings of this study highlight the potential of hemp protein hydrolysates as novel food ingredients when combined with carbohydrates, offering improved functional properties and potential health benefits.

1. Introduction

Foods are primarily composed of starch and protein, both of which play crucial roles in human nutrition. Starch is the most common carbohydrate, found in many plant-based foods such as grains, roots, and legumes (Zheng et al., 2019). The starch in flour-based foods provides ample energy, while the protein supplies essential amino acids and other nutrients necessary for the body (Amagliani et al., 2017). The combination of these two biopolymers in foods provides balanced nutrition and helps maintain human health (Wang et al., 2020; Yang et al., 2019). Globally, foods containing these components, such as bread, pasta, rice, and legumes, are staples in many diets (Li et al., 2014).

The inclusion of exogenous plant-based protein in a starch based food system not only increases the nutritional value but also enhances structural-cum-sensory attributes of the final food product (Zhang et al.,

2021). Physicochemical and functional properties of proteins such as hydration, thermal and gelation behaviors greatly impact the attributes of starch-protein blended matrices. In addition, various processing operations also influence the structural and functional behaviors of both starch and proteins, which further increase inter-molecular interactions between these two biopolymers. Enhanced interactions of starch and proteins substantially modulate the digestive, pasting, rheological, sensory, thermal and textural attributes of obtained starch-protein blended matrices (Zhang et al., 2021).

The viscoelastic matrix formed through starch-protein interactions is typically described as a particulate system, in which starch granules and/or protein aggregates (dispersed phase- a discrete sub-portion) are embedded and distributed within a porous 3-D protein biopolymer network (continuous phase) (Wang et al., 2020; Yang et al., 2019). The polymeric network is generally responsible for semi-solid, soft and moist

^{*} Corresponding authors.

E-mail addresses: lokesh.kumar@lincoln.ac.nz (L. Kumar), hannah.lee@lincoln.ac.nz (H. Lee).

<https://doi.org/10.1016/j.foostr.2026.100535>

Received 2 January 2025; Received in revised form 8 November 2025; Accepted 26 May 2026

Available online 28 May 2026

2213-3291/© 2026 The Author(s). Published by Elsevier Ltd. This is an open access article under the CC BY-NC license (<http://creativecommons.org/licenses/by-nc/4.0/>).

texture along with viscoelastic attributes of a food matrix, whereas the size and distribution of starch granules within 3-D network of proteins determines the bulk density, compressibility, and flowability of the food matrix. The findings by Guan et al. (2020) show the importance of particle size in modulating the structural and functional properties of food matrices, where different ultrafine flours significantly increased in peak, trough, breakdown and final viscosities.

In Recent years, food research emphasizes interactions within food matrices rather than isolated components, aiming to capture the concept of "food synergy" and the influence of the total matrix on health (Wang et al., 2020; Yang et al., 2019). Fourier Transform Infrared (FT-IR) spectroscopy measures light absorption, transmission, or reflection at different wavelengths in food components in order to identify functional groups and molecular structures, providing valuable insights into these interactions (Guan et al., 2020). Shao et al. (2023) reported that characteristic peaks at 1047, 1022, and 995 cm^{-1} in Chinese yam starch were associated with short-range structural order, such as double-helical sequences and hydrated crystals. However, in protein samples, the major bands were obtained at 3000–3600 cm^{-1} (intermolecular hydrogen bonding and O-H stretching vibration), 2930 cm^{-1} (C-H stretching vibration), 1655 cm^{-1} (amide I), and 1540 cm^{-1} (amide II) (Shao et al., 2023). Their study concluded that no covalent interactions exist between starch and protein, although proteins enhanced the short-range ordered structure in starch.

Food texture is a critical aspect of the sensory experience and orchestrated by a complex interplay of polysaccharides and proteins (Shao et al., 2023). These biopolymers exert significant influence on the rheological properties of food, ultimately shaping how humans perceive its texture. Polysaccharides, long-chain carbohydrates like starches, pectins and gums, are renowned for their water-holding capacity and gelling abilities (Wang et al., 2020; Yang et al., 2019). They form 3-D networks that trap water molecules, leading to increased viscosity and gelation (Shao et al., 2023). Proteins, on the other hand, contribute to texture through various mechanisms-forming elastic networks, like gluten in wheat dough, or interacting with other food components to influence viscosity and mouthfeel (Shao et al., 2023). Beyond their individual roles, specific protein-polysaccharide interactions (e.g., electrostatic forces, hydrogen bonding and hydrophobic interactions) can enhance emulsion stability, leading to a smoother and creamier texture (Gentile, 2020). Rheological properties of viscoelastic food matrices are often characterized by storage modulus (G') and loss modulus (G'') (Shao et al., 2023). The storage modulus reflects energy stored during deformation, indicating solid-like behavior, while the loss modulus represents viscous energy dissipation, indicating fluid-like behavior (Shao et al., 2023). In starch-based matrices, the incorporation of proteins can enhance G' values, reflecting a stronger gel network, and modulate G'' values depending on the protein type and concentration (Fellows, 2022; Jamilah et al., 2009).

Recent studies have reported that hemp protein and its hydrolysates possess valuable functional properties such as emulsification, foaming, and gelling, enabling their incorporation into bakery products and plant-based beverages (Liu et al., 2024; Marinopoulou et al., 2024; Rawal et al., 2024; Zhang et al., 2025). Due to their relatively high contents of hydrophobic and branched-chain amino acids, hemp protein hydrolysates can form stronger non-covalent interactions in composite food matrices, potentially influencing starch functionality and texture (Malomo & Aluko, 2015; Wang & Xiong, 2019). Furthermore, hemp protein is commonly extracted from hemp seed meal, the byproduct of hempseed oil processing, providing a sustainable source of plant protein for developing functional and eco-friendly food ingredients (Helstad et al., 2022).

Although the nutritional and functional properties of hemp seed meal protein are well known, the physicochemical properties of starches with different amylose contents combined with hydrolysates of hemp protein isolates have not been explored. This study investigated the potential of hemp protein hydrolysates as a valuable ingredient in starch

based foods and examined the impact of protein hydrolysates on starch properties. The outcome of this study offers a deeper understanding of starch-protein hydrolysate interactions and holds promise for the development of healthier, sustainable, and innovative food products.

2. Materials and methods

2.1. Materials

Hemp seed meal was kindly donated by Hemp New Zealand (Tauranga, New Zealand). Normal corn starch (S4126; 27% amylose) and waxy corn starch (S9679; 1% amylose) were purchased from Sigma-Aldrich (St. Louis, MO, USA), while high amylose corn starch Hylon VII (68% amylose) was provided by Hawkins Watts (Auckland, New Zealand). Pepsin (EC: 3.4.23.1, ≥ 250 U/mg, 35 kDa) was purchased from Fisher Scientific (Loughborough, UK). 4000 P commercial bacterial protease (*Bacillus licheniformis*; EC 3.4.21.62; ≥ 12000 U/g, alkaline protease) was supplied by Hibiscus Enzyme Solutions (Auckland, New Zealand).

2.2. Extraction and enzymatic treatment

Prior to extraction, hemp seed meal was defatted with hexane twice, each for 2 h. Afterwards, the hexane was removed using a rotary evaporator. Subsequently, the defatted hemp meal was air-dried in a fume hood at 23 °C for two days.

Hemp protein isolate (HPI) was extracted by isoelectric precipitation using the method described by Tang et al. (2006) with slight modifications. The defatted hemp meal was suspended in deionized water at 1:20 (w/v). The pH of this suspension was carefully adjusted to 10.0 using a 1 M NaOH solution, and the mixture was stirred for 2 h at 35 °C with subsequent centrifugation at 6000 \times g for 20 min. Then, the pellet was discarded, and the pH of the obtained supernatant was adjusted to pH 5.0 using 1 M HCl. This solution was left undisturbed at 4 °C overnight to facilitate protein precipitation. The resulting precipitates were recovered by centrifuging at 8000 \times g for 20 min. The obtained precipitates were washed with water thrice to eliminate any salt contamination. These protein precipitates were re-suspended and deionised with a pH adjusted to 7.0. This suspension was freeze-dried (HPI) and stored for further experiments.

The hydrolysis of HPI was conducted using two enzymes under the following conditions, with slight modifications from the previously reported methods (Malomo et al., 2015). Pepsin hydrolysis was carried out at 37 °C and pH 2.0, while bacterial protease (4000 P) hydrolysis was carried out at 55 °C and pH 10.0. HPI was suspended in deionized water to obtain a 5% (w/v) solution (5 g HPI powder in 100 mL deionized water) in a glass beaker equipped with a magnetic stirrer. Then, the dispersions were pre-incubated at the optimal catalytic temperature of each protease before pH adjustment. For the pepsin reaction mixture, the enzyme-to-substrate (E:S) ratio by weight was 2% (i.e., 0.1 g of pepsin per 5 g HPI), while for the bacterial protease reaction mixture, the E:S ratio by weight was 0.5% (i.e., 0.025 g of 4000 P per 5 g of HPI). During hydrolysis, the pH of the reaction mixtures of pepsin and 4000 P was adjusted by adding 1.0 mol/L NaOH and 1.0 mol/L HCl, respectively. Then, enzymatic reactions were terminated by adjusting the pH of the reaction mixture to 4.0, followed by immersing the reaction vessels in a boiling water bath for 10 min and subsequently cooling them in ice water. The non-hydrolyzed HPI was then separated by centrifugation at 8000 \times g for one hour at 4 °C. Finally, the resulting supernatant, containing peptides, was freeze-dried to obtain the hemp protein hydrolysates (HPH), which was stored at -20°C until further analysis.

2.3. Preparation of starch-hemp protein hydrolysate (HPH) complexes

The two hemp protein hydrolysates (hemp protein hydrolyzed with bacterial protease (HPHB) and hemp protein hydrolyzed with pepsin

(HPHP) were mixed with waxy corn starch (WCS), normal corn starch (NCS) and high amylose corn starch (HACS) at 0, 10, and 20% (w/w) ratios. The starch-HPH complex mixtures were labeled; WCS (0% HPH), WCS–10%HPHB, WCS–20%HPHB, WCS–10%HPHP, WCS–20%HPHP, NCS (0% HPH), NCS–10%HPHB, NCS–20%HPHB, NCS–10%HPHP, NCS–20%HPHP, HACS (0% HPH), HACS–10%HPHB, HACS–20%HPHB, HACS–10%HPHP and HACS–20%HPHP. The starch-HPH complexes were prepared by dissolving starch (10 g) and HPH (10% and 20% weight by starch) in 100 mL of deionized water and subjected to continuous stirring for 30 min using a magnetic stirrer. The WCS-HPH and NCS-HPH mixtures were continuously stirred at 95 °C for 20 min, and HACS-HPH mixtures were boiled for 2 h. The control samples were prepared using the same method, but no HPH was added. The suspensions were cooled down to room temperature and used as such for further characterization, while the other batch of samples was freeze-dried and further sieved through a 100-mesh sieve and sealed until further analysis.

2.4. Particle size distribution

Particle size distribution of the starch-HPH complexes was measured using a Mastersizer 3000 (Malvern Panalytical) and the following method by Govoreanu et al. (2009). The particle size was measured at a 15% obscuration range, and the mean particle size was expressed as a volume-weighted diameter $D_x(4,3)$, representing the average diameter based on the volume distribution. To account for larger particles, the diameter below which 90% of the particle volume was contained $D_x(90)$ was also recorded. Additionally, $D_x(10)$ and $D_x(50)$ represent the diameters corresponding to 10% and 50% of the cumulative particle volume, respectively.

2.5. Fourier transform infrared (FT-IR) spectroscopy

The FT-IR spectrometer (ALPHA Bruker, Germany) was used to obtain the spectra of freeze-dried, finely ground starch-HPH samples. Spectra were recorded as absorbance values averaged over 25 scans within the range of 600–4000 cm^{-1} , with a resolution of 4 cm^{-1} at room temperature. Before each measurement, background correction was performed using the built-in OPUS software (version 7.2). Subsequently, all acquired spectra were further processed using the "atmospheric compensation" function in the OPUS software.

2.6. Thermal properties

The thermal properties of starch were analysed using differential scanning calorimetry (DSC) (NETZSCH DSC 214 Polyma, NETZSCH-Gerätebau GmbH, Selb, Germany), following a previous method with some modifications (Martinez et al., 2018). Briefly, 5 mg of starch was weighed into the DSC aluminium pan, and distilled water was added to achieve a starch-to-water ratio of 1:3 (w/w, on a dry weight basis). The sample was scanned over a temperature range of 20–120 °C at a heating rate of 10 °C/min. High amylose maize starch was heated up to 150 °C to ensure complete gelatinization. The thermal behaviour during retrogradation was recorded, as enthalpy change (ΔH), onset (T_o), peak (T_p) and conclusion temperatures (T_c).

2.7. Analysis of textural properties

The method of Kumar et al. (2018) was slightly modified. Samples (prepared in Section 2.3) were transferred to 50 mL plastic bottles, and stored overnight at 4 °C. The gel hardness was measured using a TA-XT2i texture analyzer (Stable Micro Systems Ltd, Surrey, UK) equipped with Texture Expert software and a 5 kg load. At room temperature, the samples were compressed to a distance of 10 mm using a cylindrical plunger (p/5) at a constant crosshead speed of 1.00 mm/s, performing a single compression cycle. All tests were carried out in triplicates.

2.8. Rheological measurements

The rheological properties of the samples were evaluated using a rheometer (MCR 302, Anton Paar, Austria), following a slightly modified method described by Luo et al. (2020). Freshly prepared starch-HPH complexes were allowed to cool at room temperature (25 °C) for two hours prior to analysis. Measurements were performed using a parallel plate geometry (PP50/SN) with a plate diameter of 25 mm and a gap of 1 mm. After a 3-minute equilibration period, rheological characteristics were conducted. Amplitude sweep tests were performed to determine the storage modulus (G') and loss modulus (G'') as functions of strain (0.01–1000%) at a constant frequency of 1 Hz. Subsequently, frequency sweep tests were carried out over an angular frequency range of 1–100 rad/s at a constant strain of 1%, which was confirmed to fall within the linear viscoelastic region based on the amplitude sweep results.

2.9. Statistical analysis

All the experiments were performed in triplicates and represented as means \pm standard deviation. The statistical significance of the data set was analysed through Tukey's test using one-way ANOVA analysis (Minitab 19, Minitab Ltd., Sydney, Australia). Origin Pro (2023) software was used to make figures.

3. Results and discussion

3.1. Particle size distribution of starch-hemp protein hydrolysate complexes

The data presented in Fig. 1 and Table 1 provide insights into the particle size distribution of mixtures of starch and hydrolysates, elucidating the effects of HPHB and HPHP on the structure of corn starch with varying amylose content. Adding hydrolysates significantly increased the particle size of corn starch, with all samples exhibiting a unimodal particle distribution (Table 1 and Fig. 1). Specifically, the NCS-HPH and WCS-HPH mixtures were predominantly falling within the 10–100 μm range, while HACS-HPH mixtures were mainly distributed within the 2–100 μm range. Table 1 shows that the addition of higher levels of hydrolysate to starch broadens the particle size distribution of the mixtures, consistent with a previous report (Ji, 2018). This indicates that hydrolysates influence the structure of corn starch.

From Fig. 1, it can be observed that the particle size increased after the addition of hydrolysates, which was particularly significant in HACS with a relatively larger particle size. In native control samples, the particle size was relatively small, reflecting good dispersibility and finer particles of untreated starch granules. However, the addition of 10% and 20% HPHB and HPHP resulted in a significant increase in particle size, notably for NCS–20% HPHB and NCS–20% HPHP, as evidenced by $D_x(10)$, $D_x(50)$, and $D_x(90)$ values. A potential explanation for this increase is moisture absorption and the subsequent expansion of starch granules, leading to cross-linking between starch granules and hydrolysates, thus, increasing the granule size. Although the addition of HPHB and HPHP also increased the particle size of other starch samples, the magnitude of this increase was less pronounced compared to HACS samples. This suggests that the amylose content in the mixtures significantly affects the impact of hydrolysates. Table 1 shows that the $D_x(10)$ values for untreated samples were relatively low, particularly for Native-HACS (5.42 μm), indicating a higher proportion of small particles. In contrast, the $D_x(10)$ values for NCS–20% HPHP (26.54 μm) and WCS–20% HPHP (25.76 μm) were higher, suggesting larger small particles post hydrolysate addition. The $D_x(50)$ values revealed that the median particle size was largest for NCS–20% HPHB (69.62 μm) and HACS–20% HPHB (77.82 μm), indicating larger median particles in these samples, especially in high amylose starch after hydrolysate addition. For $D_x(90)$, HACS–20% HPHB (771.4 μm) and HACS–10%

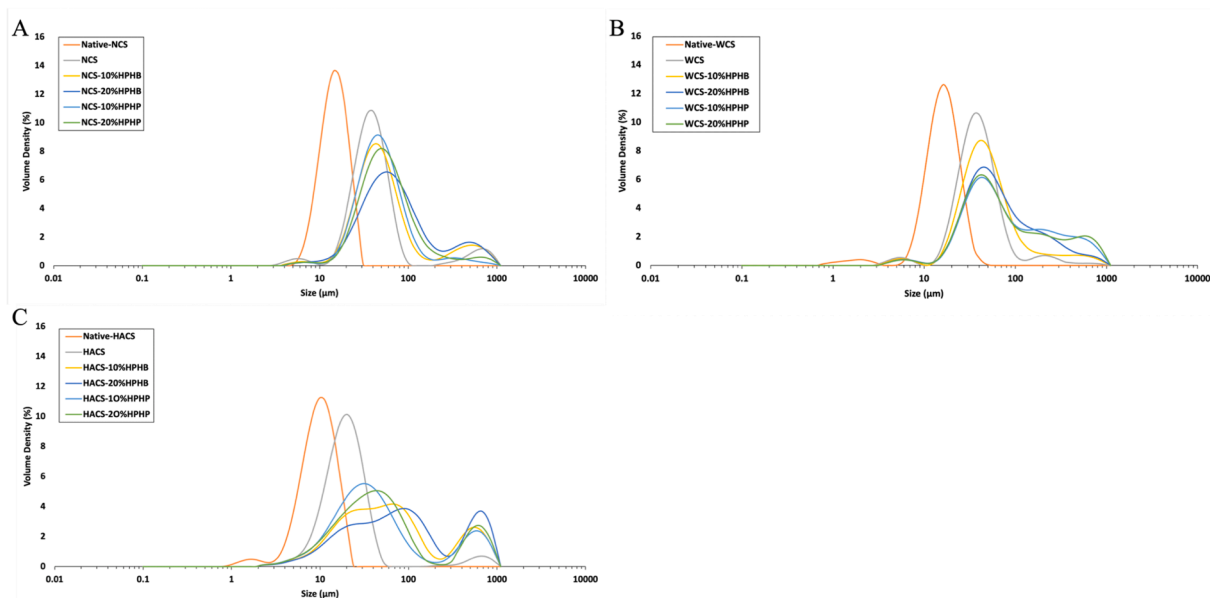


Fig. 1. Particle size distribution of starch-hemp protein hydrolysates (HPH).

Table 1

Particle size distribution of starch-hemp protein hydrolysates (HPH) (N = 3).

Samples	Dx (10)	Dx (50)	Dx (90)	Dx (4,3)
*Native-NCS	9.37 ± 0.38 ^m	15.47 ± 0.70 ^{kl}	24.78 ± 2.59 ^h	26.47 ± 22.27 ^j
NCS	22.14 ± 0.21 ^h	41.74 ± 1.08 ^{ij}	289.2 ± 205.8 ^d	107.34 ± 19.41 ^{ef}
NCS–10% HPHB	25.43 ± 1.17 ^{ef}	53.52 ± 4.16 ^{ef}	319.8 ± 119.7 ^d	118.34 ± 19.66 ^e
NCS–20% HPHB	26.08 ± 0.27 ^{ab}	69.62 ± 1.51 ^b	402.44 ± 31.74 ^c	140.22 ± 5.62 ^d
NCS–10% HPHP	24.94 ± 0.58 ^{de}	50.74 ± 4.07 ^{gh}	116.24 ± 26.20 ^{efg}	74.25 ± 12.44 ^h
NCS–20% HPHP	26.54 ± 0.45 ^a	57.37 ± 3.09 ^{de}	152.60 ± 19.04 ^{ef}	92.89 ± 4.69 ^{fg}
*Native-WCS	9.75 ± 0.09 ^{lm}	16.90 ± 0.63 ^k	27.48 ± 2.13 ^h	17.70 ± 0.92 ^j
WCS	21.59 ± 0.21 ^h	40.29 ± 1.44 ^j	84.56 ± 18.21 ^{fgh}	54.46 ± 9.83 ⁱ
WCS–10% HPHB	23.73 ± 0.52 ^g	47.22 ± 2.64 ^{gh}	182.7 ± 96.2 ^e	90.60 ± 17.85 ^{fgh}
WCS–20% HPHB	23.92 ± 0.89 ^{fg}	51.55 ± 3.23 ^{fg}	179.3 ± 40.84 ^e	87.26 ± 8.23 ^{gh}
WCS–10% HPHP	25.30 ± 1.14 ^{cd}	62.65 ± 9.93 ^{cd}	419.6 ± 50.6 ^c	146.65 ± 15.99 ^{cd}
WCS–20% HPHP	25.76 ± 0.68 ^{bc}	66.23 ± 7.49 ^{bc}	505.05 ± 25.74 ^b	165.35 ± 7.66 ^b
*Native-HACS	5.42 ± 0.08 ⁿ	10.28 ± 0.05 ^l	17.30 ± 0.17 ^h	10.82 ± 0.06 ^j
HACS	10.20 ± 0.12 ^l	20.48 ± 0.20 ^k	39.19 ± 2.39 ^{gh}	49.81 ± 13.82 ⁱ
HACS–10% HPHB	13.76 ± 0.70 ^j	59.90 ± 11.62 ^d	542.8 ± 99.3 ^b	160.9 ± 24.41 ^{bc}
HACS–20% HPHB	14.69 ± 0.27 ^j	77.82 ± 6.91 ^a	771.4 ± 41.06 ^a	220.3 ± 18.09 ^a
HACS–10% HPHP	12.42 ± 0.49 ^k	39.57 ± 4.11 ^j	531.3 ± 83.1 ^b	139.65 ± 21.38 ^d
HACS–20% HPHP	12.44 ± 0.20 ^k	46.02 ± 2.06 ^{hi}	583.5 ± 54.0 ^b	154.2 ± 17.79 ^{bcd}

Means in a column with different superscript letters are significantly different ($p < 0.05$). HPHB-hemp protein hydrolyzed by bacterial protease, HPHP-hemp protein hydrolyzed by pepsin NCS-normal corn starch, WCS-waxy corn starch, HACS-high amylose corn starch. *Native starch refers to starch that has not undergone any heat treatment.

HPHB (542.8 μm) showed significantly larger particles. Similarly, Dx (4,3) values were highest for HACS–20% HPHB (220.3 μm) and HACS–10% HPHB (160.9 μm), highlighting the substantial effect of hydrolysates on overall particle size in cooked high amylose starch samples.

Adding both HPHB and HPHP at 10% and 20% levels led to a significant increase in particle size, with 20% HPHB having a more pronounced effect. Moreover, the particle size of HACS increased notably following hydrolysate addition, indicating that higher amylose content amplifies the impact on particle size. This analysis reveals that hydrolysates, particularly at higher concentrations, markedly influence the particle size distribution of starches, with high amylose starch being more sensitive to these changes.

3.2. FT-IR analysis

The FT-IR spectra for starch-HPH are shown in Fig. 2. Pronounced peaks were observed in the range of 950–1100 cm^{-1} , 1500–1750 cm^{-1} ,

and 2750–3750 cm^{-1} for the mixtures. Compared to control, the absorption peaks and positions in the starch-HPH mixtures were similar, with no disappearance or appearance of new peaks, indicating the absence of new functional groups in the mixtures. This suggests that there were no covalent interactions between starch and HPHB and HPHP. The absorption peak of N-H was at 1520 cm^{-1} (Table 2), which is attributed to specific protein components, amide I (1580–1720 cm^{-1}) and amide II (1480–1580 cm^{-1}) (López-Barón et al., 2018). Samples containing HPH exhibited characteristic peaks in the amide II region at 1570 cm^{-1} , with peak intensity gradually increasing with the addition of HPH.

Around the wavenumber of 1650 cm^{-1} (Table 2), typical protein spectra were associated with the stretching vibration of the C=O bond in the amide groups. In NCS and WCS, with the addition of HPH, the C=O absorption peak gradually shifted from a lower wavenumber to a higher wavenumber, with 20% HPHP being the most significant. In comparison to NCS and WCS, the shift from a lower to a higher wavenumber in HACS was not significant, and no change was observed

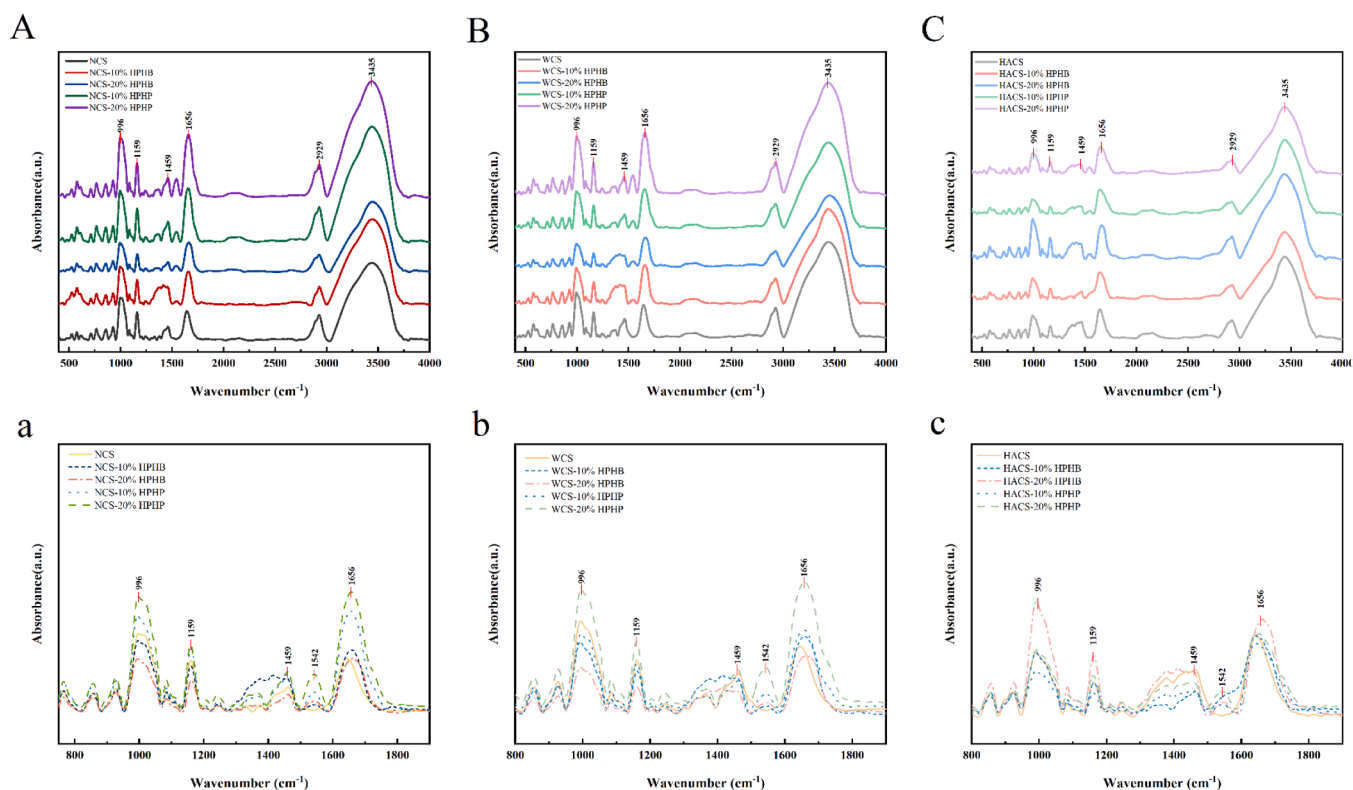


Fig. 2. FT-IR spectra of normal corn starch-hemp protein hydrolysate complexes (A), waxy corn starch-hemp protein hydrolysate complexes (B), and high amylose corn starch-hemp protein hydrolysate complexes (C), and deconvoluted FT-IR spectra of normal corn starch-hemp protein hydrolysate complexes (a), waxy corn starch-hemp protein hydrolysate complexes (b) and high amylose corn starch-hemp protein hydrolysate complexes (c).

Table 2
Characteristic FT-IR band interpretations observed in starch-HPH complexes.

Observed peak (cm ⁻¹)	Component	Band interpretation	Source
996	Starch	C–O stretching (α -1,4 glycosidic linkages; ordered or crystalline starch regions)	(Kizil et al., 2002)
1159	Starch	C–O–C and C–O stretching (glycosidic linkages in polysaccharides)	(Kizil et al., 2002)
1549	Protein	Amide II (N–H bending and C–N stretching of peptide bonds)	(Socrates, 2004)
1656	Protein	Amide I (C=O stretching of peptide bonds; protein secondary structure)	(Socrates, 2004)
2929	Protein / Starch	C–H stretching (aliphatic –CH ₂ and –CH ₃ groups)	(Kizil et al., 2002)
3405	Starch / Protein	O–H stretching (hydrogen-bonded hydroxyl groups; intermolecular hydrogen bonding)	(Socrates, 2004)

similar to the previously reported shift of the C=O absorption peak from a higher to a lower wavenumber in mixtures of high amylose corn starch and soy hydrolyzed protein (Zhu et al., 2022). In the FT-IR spectrum (Table 2), the band between 3000 and 3600 cm⁻¹ was related to the O-H stretching vibration. The shift of this peak towards lower wavenumbers indicates an enhancement of hydrogen bonds in the system, while the shift towards higher wavenumbers indicates a weakening of hydrogen bonds in the system (Kizil et al., 2002; Lu et al., 2021).

For NCS and WCS with lower content of amylose starch, the addition of 10%/20% HPHB did not result in a significant shift in the -OH absorption peak, indicating its minimal influence on the -OH stretching vibration of the complex. In contrast, the addition of 10%/20% HPHB caused a shift towards higher wavenumbers, with 20% HPHB showing

the most pronounced effect. This shift is likely due to the enhanced non-covalent interactions between 10% and 20% HPHB and HACS, which suppresses the interactions between starch molecules, leading to the shift in the -OH peak. In the HACS, it was observed that the addition of 10%/20% HPHB did not alter the -OH absorption peak, while the addition of 10%/20% HPHB caused a shift towards lower wavenumbers, with 20% HPHB exhibiting the most significant effect. Interestingly, the addition of HPHB significantly reduced the height of the -OH peak in the HACS-HPH, indicating that the addition of HPHB may disrupt the hydrogen bonds between starch molecules (Zhu et al., 2020). In contrast, the addition of HPHB increased the height of the -OH peak in the NCS and WCS mixtures, possibly enhancing the hydrogen bonds between starch molecules. In addition, the weakened absorption band around 996 cm⁻¹ further indicated a reduction in the degree of crystallinity, suggesting that HPHB incorporation disrupted the ordered structure of starch.

3.3. Thermal properties of retrograded starch

The thermal properties of NCS, WCS, and HACS were significantly influenced by the addition of hemp protein hydrolysates (HPHB and HPHB). Gelatinization temperatures (To, Tp, Tc) and enthalpy (ΔH) varied substantially between starch types and in response to the type and concentration of hydrolysate (Table 3).

HACS demonstrated the highest thermal stability of the starches (Table 3), as evidenced by its elevated gelatinization temperatures (To, Tp, Tc) compared to NCS and WCS. For example, native HACS exhibited a To of 69.15°C, while NCS and WCS showed lower To values of 65.95°C and 68.85°C, respectively. This enhanced thermal stability of HACS can be attributed to its higher amylose content, which requires greater thermal energy to disrupt its crystalline structure (Li et al., 2021). The addition of protein hydrolysates further amplified these thermal properties, particularly in HACS. Specifically, HACS with 20% HPHB showed

Table 3

DSC parameters including To (°C), Tp (°C), Tc (°C), Tc-To (°C) and ΔH (J/g) for starch-hemp protein hydrolysates (N = 3).

Sample	To	Tp	Tc	Tc-To	ΔH
Native-NCS	65.95 ± 0.35 ^g	70.50 ± 0.14 ^f	75.55 ± 0.07 ^c	9.60 ± 0.28 ^c	11.60 ± 0.49 ^{abcde}
NCS–10% HPHB	67.90 ± 0.14 ^f	72.60 ± 0.14 ^{ef}	77.40 ± 0.14 ^c	9.50 ± 0.28 ^c	10.13 ± 0.13 ^{cde}
NCS–20% HPHB	68.85 ± 0.35 ^{cdef}	73.60 ± 0.14 ^{cde}	78.60 ± 0.14 ^c	9.75 ± 0.21 ^c	9.76 ± 0.01 ^{ef}
NCS–10% HPHP	68.00 ± 0.28 ^{ef}	72.85 ± 0.35 ^{def}	77.65 ± 0.07 ^c	9.65 ± 0.21 ^c	12.43 ± 0.46 ^{ab}
NCS–20% HPHP	68.60 ± 0.00 ^{def}	73.60 ± 0.14 ^{cde}	79.00 ± 0.00 ^c	10.40 ± 0.00 ^c	12.22 ± 0.39 ^{ab}
Native-WCS	68.85 ± 0.21 ^{cdef}	73.1 ± 0.14 ^{cde}	77.6 ± 0.28 ^c	8.75 ± 0.07 ^c	13.20 ± 0.07 ^a
WCS–10% HPHB	69.70 ± 0.14 ^{bcd}	74.15 ± 0.07 ^{cde}	78.75 ± 0.07 ^c	9.05 ± 0.21 ^c	11.14 ± 0.06 ^{bcd}
WCS–20% HPHB	70.75 ± 0.21 ^{ab}	75.30 ± 0.42 ^c	79.85 ± 0.64 ^c	9.10 ± 0.42 ^c	10.00 ± 0.22 ^{def}
WCS–10% HPHP	70.05 ± 0.21 ^{abc}	74.45 ± 0.21 ^{cde}	78.85 ± 0.07 ^c	8.80 ± 0.14 ^c	11.88 ± 0.11 ^{abcd}
WCS–20% HPHP	70.65 ± 0.21 ^{ab}	75.20 ± 0.14 ^{cd}	79.55 ± 0.49 ^c	8.90 ± 0.28 ^c	10.98 ± 0.13 ^{bcd}
Native- HACS	69.15 ± 0.21 ^{cde}	80.45 ± 0.64 ^{ab}	94.25 ± 0.49 ^b	25.10 ± 0.28 ^b	12.08 ± 0.39 ^{abc}
HACS–10% HPHB	70.45 ± 0.35 ^{ab}	78.65 ± 0.21 ^b	105.40 ± 0.28 ^a	34.95 ± 0.64 ^a	7.59 ± 0.82 ^g
HACS–20% HPHB	70.70 ± 0.85 ^{ab}	79.15 ± 1.34 ^b	104.45 ± 0.92 ^a	33.75 ± 1.77 ^a	6.58 ± 0.17 ^g
HACS–10% HPHP	71.15 ± 0.07 ^a	81.95 ± 1.12 ^a	103.90 ± 1.56 ^a	32.75 ± 1.48 ^a	10.00 ± 1.14 ^{def}
HACS–20% HPHP	71.05 ± 0.07 ^a	80.10 ± 1.13 ^{ab}	103.25 ± 4.56 ^a	32.20 ± 4.53 ^a	7.99 ± 0.31 ^{fg}

Means in a column with different superscript letters are significantly different ($p < 0.05$).

a marked increase in Tp to 80.1°C and Tc to 103.25°C, suggesting that interactions between HPHB and HACS led to even greater thermal stability. Studies reported that electrostatic interactions between starch molecules within granules, along with the amphiphilic properties of amino acids, can significantly modify the thermal properties of starch (Lockwood et al., 2008). Similar research has shown that the incorporation of amino acids notably elevates the To, Tp, and Tc values of starch (Ito et al., 2006). This effect is likely due to the electrostatic interactions between the starch granules and amino acids, which require higher temperatures to break down the molecular structure of the starch chains.

The gelatinization range (Tc-To) also varied significantly across the starch samples, with HACS displaying the widest range, especially in the presence of HPHB. For instance, HACS with 20% HPHB exhibited a gelatinization range of 32.2°C, while native NCS had a much narrower range of 9.6°C. This broader gelatinization range in HACS indicates stronger molecular interactions between HPHB and amylose, likely resulting in greater structural modifications and an extended temperature range for gelatinization. These interactions may involve the formation of stabilizing bonds between the hydrolysates and starch chains, delaying gelatinization and enhancing the stability of the starch matrix.

The ΔH (reflects the thermal energy needed to gelatinize starch crystallites) decreased consistently with the addition of protein hydrolysates, particularly at higher concentrations. For example, the ΔH of HACS with 20% HPHB decreased from 12.08 J/g (native HACS) to 6.58 J/g, indicating that less energy was required to gelatinize the starch in the presence of protein hydrolysates. This reduction in ΔH suggests that the hydrolysates disrupted the crystalline regions of the starch, facilitating easier gelatinization. Other starch-protein/hydrolysate mixtures also reported similar results (Ji, 2020; Pang et al., 2022; Song et al., 2024; Zhu et al., 2022). While this trend was observed across all starch types, it was particularly shown in HACS, where the addition of hydrolysates had a significant impact on the energy required for gelatinization.

3.4. Texture properties

The textural parameters (elasticity, hardness, and adhesiveness) of starch-hydrolysate complexes were analysed using a texture analyser, and the findings are provided in Table 4. Gel formation is mainly affected by amylose gelation and different percentages of protein hydrolysates. The influence of hydrolysates alters the molecular structure of starch, thereby affecting its physical properties. Among all samples, HACS and HACS–10%HPHB exhibited the highest mean elasticity values, both at 0.10 N-s, whereas NCS–10%HPHB showed the highest mean hardness at 0.59 N. For adhesiveness, NCS had the most negative mean value at –0.16 N for adhesiveness.

The addition of HPHB increased the elasticity of NCS and WCS while showing a decreasing trend in HACS. Similarly, the addition of HPHB increased the elasticity of WCS but significantly decreased that of HACS, with no significant change observed in NCS. WCS–20%HPHB showed an approximately 28% increase in elasticity compared to the control group, while HACS–20%HPHB exhibited a decrease of about 50%. It is evident that the addition of HPHB and HPHB can enhance the elasticity of the mixture, despite a reduction of HACS. Regarding hardness, the effect of HPHB addition mirrored elasticity, significantly increasing the hardness of normal and waxy starches but decreasing that of HACS.

Conversely, the addition of HPHB reduced the hardness of NCS and HACS but increased that of WCS. HACS–20%HPHB showed a decrease of about 51% in hardness, while WCS–20%HPHB exhibited an increase of about 125%. The hardness of starch gel is mainly influenced by starch retrogradation (Zhu & Cui, 2020). Retrogradation is a process in which the ratio of amylose and amylopectin in starch is crucial. As the content of amylose increases, the rate of retrogradation accelerates, thereby increasing the hardness of the starch gel (Li et al., 2016). This phenomenon was particularly evident in the control group. Interestingly, with an increase in hydrolysate, a significant decrease in hardness was observed in HACS mixtures. This may be because hydrolysate products may inhibit starch retrogradation, thereby delaying product aging and resulting in lower hardness. For adhesiveness, the influence of 20% HPHB on WCS was the most significant. WCS–20%HPHB showed the most significant increase in adhesiveness, approximately 114%, and the most significant decrease was observed in HACS–20%HPHB, with a decrease of about 60%. From these results, it can be seen that the addition of 10%/20% HPHB and 10%/20% HPHB in NCS and WCS increased the cross-linking degree of starch, with 10% HPHB being the most significant, thereby increasing the elasticity and hardness of the samples (except for the elasticity in NCS with 10%/20% HPHB). In WCS, the increase in viscosity was most notable with 20%HPHB. This change

Table 4

Gel textural properties of starch mixtures (N = 3).

Samples	Elasticity (N-s)	Hardness (N)	Adhesiveness (N)
NCS	0.06 ± 0.01 ^{def}	0.32 ± 0.03 ^{cd}	–0.16 ± 0.03 ^g
NCS–10%HPHB	0.07 ± 0.01 ^{bcd}	0.59 ± 0.06 ^a	–0.14 ± 0.03 ^{cdefg}
NCS–20%HPHB	0.07 ± 0.01 ^{bcd}	0.56 ± 0.06 ^{ab}	–0.13 ± 0.04 ^{cdefg}
NCS–10%HPHP	0.06 ± 0.01 ^{def}	0.39 ± 0.05 ^{cd}	–0.14 ± 0.03 ^{efg}
NCS–20%HPHP	0.06 ± 0.01 ^{def}	0.37 ± 0.03 ^d	–0.13 ± 0.02 ^{cdef}
WCS	0.07 ± 0.02 ^{cde}	0.24 ± 0.03 ^{ef}	–0.07 ± 0.01 ^{ab}
WCS–10%HPHB	0.08 ± 0.01 ^{bcd}	0.57 ± 0.05 ^{ab}	–0.14 ± 0.05 ^{defg}
WCS–20%HPHB	0.08 ± 0.01 ^{bcd}	0.45 ± 0.04 ^c	–0.15 ± 0.03 ^{fg}
WCS–10%HPHP	0.08 ± 0.01 ^{bcd}	0.44 ± 0.07 ^c	–0.14 ± 0.04 ^{efg}
WCS–20%HPHP	0.09 ± 0.01 ^{abc}	0.54 ± 0.09 ^b	–0.10 ± 0.02 ^{bcd}
HACS	0.10 ± 0.03 ^a	0.41 ± 0.08 ^{cd}	–0.10 ± 0.03 ^{bcd}
HACS–10%HPHB	0.07 ± 0.01 ^{cde}	0.30 ± 0.06 ^e	–0.06 ± 0.02 ^a
HACS–20%HPHB	0.05 ± 0.01 ^f	0.20 ± 0.05 ^f	–0.04 ± 0.01 ^a
HACS–10%HPHP	0.10 ± 0.05 ^{ab}	0.27 ± 0.06 ^e	–0.12 ± 0.02 ^{cdef}
HACS–20%HPHP	0.06 ± 0.03 ^{def}	0.23 ± 0.05 ^{ef}	–0.10 ± 0.01 ^{bc}

Means in a column with different superscript letters are significantly different ($p < 0.05$). HPHB-hemp protein hydrolyzed by bacterial protease, HPHB-hemp protein hydrolyzed by pepsin, NCS-normal corn starch, WCS-waxy corn starch, HACS-high amylose corn starch.

may be related to the surface chemical properties and molecular interactions induced by the protein hydrolysates. Moreover, particle size distribution results corroborate these findings.

Different hydrolysates and their concentrations significantly impact the textural properties of starch gels. Addition of HPH and HPHB enhanced the elasticity and hardness of WCS and NCS gels, while improving the adhesiveness of WCS gel. Notably, the effects were most pronounced with the addition of 20%HPHP on WCS gel elasticity, 10% HPHB on WCS gel hardness, and 20%HPHB on WCS gel adhesiveness.

3.5. Rheological analysis

The changes in storage modulus (G') are commonly used as an indicator to monitor starch gelatinization (Li et al., 2017). Both storage modulus (G') and loss modulus (G'') of all samples were dependent on frequency, and the addition of HPH significantly changed the storage modulus (G'). After the addition of protein hydrolysate, NCS exhibited greater viscosity and was the most stable, followed by WCS, and HACS being the least stable (Fig. 3 and Fig. 4). The results also indicate that the addition of HPH affected the gel structure of starch. Figs. 3 and 4 show that the G' and G'' of all samples increased with increasing frequency, and the addition of HPH significantly changed both G' and G'' . Moreover, all G' values were higher than G'' , indicating that all samples exhibited characteristics typical of weak gels (Luo et al., 2020). It is evident that the addition of HPHB and HPH in NCS-HPH increased both G' and G'' , while in WCS-HPH and HACS-HPH, the addition of HPHB and HPH reduced both G' and G'' (Figs. 3 and 4), indicating a reduction in the starch paste's elastic properties. This is attributed to the interaction

between HPH and leached amylose, which delays the re-aggregation of amylose molecules (Yang et al., 2021).

Interestingly, different concentrations of HPHB and HPH had varying effects on three different types of starch. In NCS-HPH, the addition of 10% HPH showed the most significant impact on NCS. However, in WCS-HPH, the addition of 10% HPH decreased both G' and G'' , whereas the addition of 10% HPHB increased these values. This effect could be attributed to the low amylose content of the starch, which inherently leads to the development of weaker interactions between starch molecules. HPHB may further interfere with these weak interactions, leading to a decrease in storage modulus (G'). Starch contains numerous hydroxyl groups in both branched and linear chains. These hydroxyl groups can form hydrogen bonds with the amino acid residues in protein hydrolysates, promoting close associations between starch molecules and protein hydrolysates, and thereby enhancing the stability and strength of the gel network.

However, in HACS-HPH, it is found that regardless of the concentration of HPH, both G' and G'' decreased, with the most significant decrease observed with 20% HPHB. This could be due to the entanglement between high amylose content starch and peptide chains. This decrease may also be attributed to 20% HPHB encapsulating most of the starch particles, thereby limiting the diffusion of amylose molecules into the starch paste, reducing the number of interactions between amylose molecules, and thus inhibiting the formation of elastic gels (Ma et al., 2019). This has also been confirmed from textural properties. In contrast to previous studies (Luo et al., 2020; Ma et al., 2019; Xiao et al., 2020), no increase in G' and G'' with increasing additive concentration was observed. This could be because a high concentration of protein

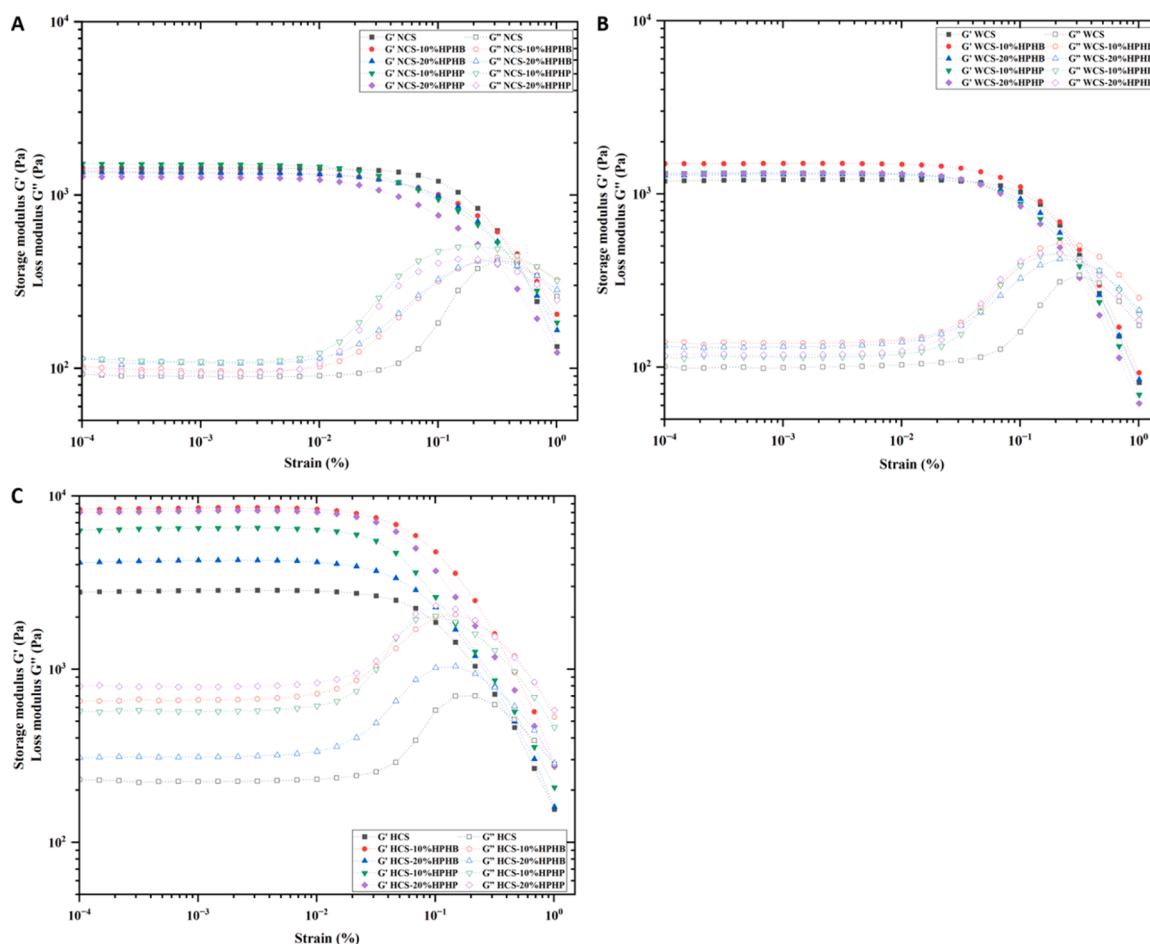


Fig. 3. Amplitude sweep parameters (Storage modulus (G') and Loss modulus (G'')) for the (A) NCS-HPH complex, (B) WCS-HPH complex, and HACS-HPH complex.

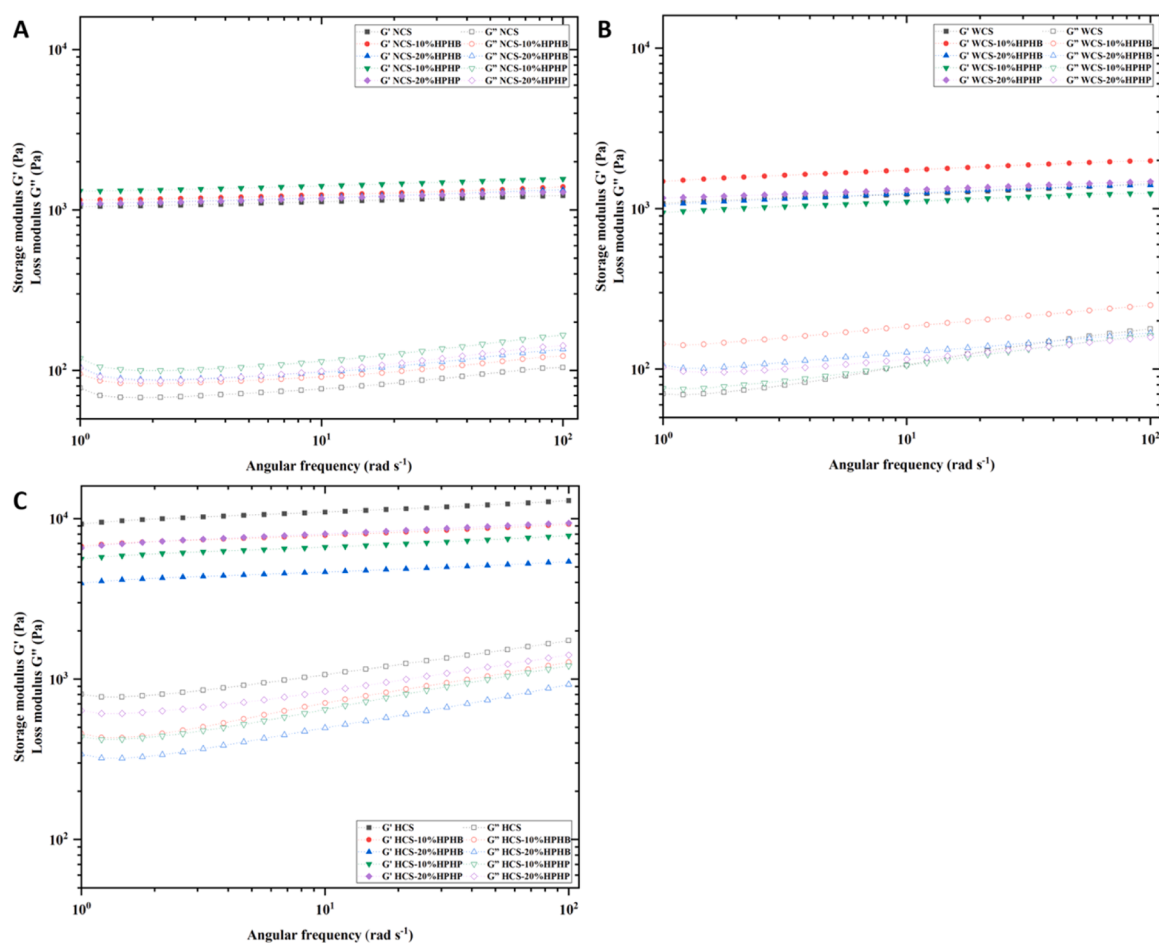


Fig. 4. Frequency sweep parameters (Storage modulus (G') and Loss modulus (G'')) for the (A) NCS-HPH complex, (B) WCS-HPH complex, and HACS-HPH complex.

hydrolysates may have an adverse effect, disrupting the interactions between starch molecules and leading to a decrease in storage modulus (G').

4. Conclusion

This study examined the effects of hemp protein hydrolysates (HPH), produced by pepsin and bacterial protease, on the particle size distribution, structural, textural, rheological and thermal properties of various corn starches (normal corn starch (NCS), waxy corn starch (WCS), and high amylose corn starch (HACS)). The incorporation of HPH significantly influenced the textural properties of starch gels, enhancing elasticity and hardness in NCS and WCS, while increasing adhesiveness in NCS and HACS. Notable effects were observed with 20% HPHP (hemp protein hydrolyzed by pepsin) on the elasticity of WCS, 10% HPHB (hemp protein hydrolyzed by bacterial protease) on the hardness of WCS, and 20% HPHB on the adhesiveness of WCS. Particle size analysis revealed a significant increase in granule size following hydrolysate addition, particularly in HACS, which was attributed to moisture absorption and granule expansion. Fourier transform infrared spectroscopy indicated no formation of new functional groups; however, shifts in absorption peaks suggested modifications in hydrogen bonding interactions. Rheological measurements showed that both the storage modulus (G') and loss modulus (G'') were significantly affected, with variations depending on starch type and hydrolysate concentration. Specifically, G' and G'' increased in NCS-HPH mixtures but generally decreased in WCS-HPH and HACS-HPH systems. Additionally, the incorporation of HPH, particularly HPHP, markedly altered the thermal properties of the starches, especially HACS. Overall, these findings

suggest that integrating hemp protein hydrolysates into starch-based foods can enhance their functional and nutritional properties, offering potential applications in the development of nutrient-rich functional foods.

CRediT authorship contribution statement

Hannah Lee: Writing – review & editing, Validation, Supervision, Resources, Project administration, Methodology, Conceptualization.
Lokesh Kumar: Writing – review & editing, Validation, Supervision, Resources, Project administration, Methodology, Conceptualization.
Gaosheng Wu: Writing – review & editing, Writing – original draft, Visualization, Software, Methodology, Investigation, Formal analysis, Data curation, Conceptualization.
James D. Morton: Writing – review & editing, Supervision, Conceptualization.

Declaration of Competing Interest

We are pleased to declare that there is no conflict of interest between the authors. This submission has not been submitted for consideration elsewhere.

References

- Amagliani, L., O'Regan, J., Kelly, A. L., & O'Mahony, J. A. (2017). The composition, extraction, functionality and applications of rice proteins: A review. *Trends in Food Science & Technology*, 64, 1–12. <https://doi.org/10.1016/j.tifs.2017.01.008>
- Fellows, P. J. (2022). *Food processing technology: principles and practice*. Woodhead publishing.
- Gentile, L. (2020). Protein–polysaccharide interactions and aggregates in food formulations. *Current Opinion in Colloid & Interface Science*, 48, 18–27.

- Govoreanu, R., Saveyn, H., Van Der Meer, P., Nopens, I., & Vanrolleghem, P. A. (2009). A methodological approach for direct quantification of the activated sludge floc size distribution by using different techniques. *Water Science and Technology*, 60(7), 1857–1867. <https://doi.org/10.2166/wst.2009.535>
- Guan, E., Yang, Y., Pang, J., Zhang, T., Li, M., & Bian, K. (2020). Ultrafine grinding of wheat flour: Effect of flour/starch granule profiles and particle size distribution on falling number and pasting properties. *Food Science & Nutrition*, 8(6), 2581–2587.
- Helstad, A., Forsén, E., Ahlström, C., Mayer Labba, I. C., Sandberg, A. S., Rayner, M., & Purhagen, J. K. (2022). Protein extraction from cold-pressed hempseed press cake: From laboratory to pilot scale. *Journal of Food Science*, 87(1), 312–325. <https://doi.org/10.1111/1750-3841.16005>
- Ito, A., Hattori, M., Yoshida, T., & Takahashi, K. (2006). Contribution of the net charge to the regulatory effects of amino acids and epsilon-poly (L-lysine) on the gelatinization behavior of potato starch granules. *Bioscience, Biotechnology, and Biochemistry*, 70(1), 76–85. <https://doi.org/10.1271/bbb.70.76>
- Jamilah, B., Mohamed, A. Z., Abbas, K. A., Rahman, R. b A., Karim, R., & Hashim, D. M. (2009). Protein-starch interaction and their effect on thermal and rheological characteristics of a food system: A review. *Journal of Food Agriculture & Environment*, 7, 169–174.
- Ji, Y. (2018). *in vitro* digestion and physicochemical characteristics of corn starch mixed with amino acid modified by low pressure treatment. *Food Chemistry*, 242, 421–426. <https://doi.org/10.1016/j.foodchem.2017.09.073>
- Ji, Y. (2020). Effect of annealing on the functional properties of corn starch/corn oil/lysine blends. *International Journal of Biological macromolecules*, 144, 553–559. <https://doi.org/10.1016/j.ijbiomac.2019.12.122>
- Kizil, R., Irudayaraj, J., & Seetharaman, K. (2002). Characterization of irradiated starches by using FT-Raman and FTIR spectroscopy. *Journal of Agricultural and Food Chemistry*, 50(14), 3912–3918.
- Kumar, L., Brennan, M., Zheng, H., & Brennan, C. (2018). The effects of dairy ingredients on the pasting, textural, rheological, freeze-thaw properties and swelling behaviour of oat starch. *Food Chemistry*, 245, 518–524. <https://doi.org/10.1016/j.foodchem.2017.10.125>
- Li, C., Hu, Y., & Li, E. (2021). Effects of amylose and amylopectin chain-length distribution on the kinetics of long-term rice starch retrogradation. *Food Hydrocolloids*, 111, Article 106239. <https://doi.org/10.1016/j.foodhyd.2020.106239>
- Li, Q.-Q., Wang, Y.-S., Chen, H.-H., Liu, S., & Li, M. (2017). Retardant effect of sodium alginate on the retrogradation properties of normal cornstarch and anti-retrogradation mechanism. *Food Hydrocolloids*, 69, 1–9. <https://doi.org/10.1016/j.foodhyd.2017.01.016>
- Li, S., Wei, Y., Fang, Y., Zhang, W., & Zhang, B. (2014). DSC study on the thermal properties of soybean protein isolates/corn starch mixture. *Journal of Thermal Analysis and Calorimetry*, 115, 1633–1638.
- Li, W., Li, C., Gu, Z., Qiu, Y., Cheng, L., Hong, Y., & Li, Z. (2016). Retrogradation behavior of corn starch treated with 1,4- α -glucan branching enzyme. *Food Chemistry*, 203, 308–313. <https://doi.org/10.1016/j.foodchem.2016.02.059>
- Liu, X., Xue, F., & Adhikari, B. (2024). Recent advances in plant protein modification: spotlight on hemp protein. *Sustainable Food Technology*, 2(4), 893–907.
- Lockwood, S., King, J. M., & Labonte, D. R. (2008). Altering Pasting Characteristics of Sweet Potato Starches through Amino Acid Additives. *Journal of Food Science*, 73(5), C373–C377. <https://doi.org/10.1111/j.1750-3841.2008.00755.x>
- López-Barón, N., Sagnelli, D., Blennow, A., Holse, M., Gao, J., Saaby, L., Müllertz, A., Jespersen, B., & Vasanthan, T. (2018). Hydrolysed pea proteins mitigate *in vitro* wheat starch digestibility. *Food Hydrocolloids*, 79, 117–126. <https://doi.org/10.1016/j.foodhyd.2017.12.009>
- Lu, X., Chang, R., Lu, H., Ma, R., Qiu, L., & Tian, Y. (2021). Effect of amino acids composing rice protein on rice starch digestibility. *Food Science & Technology*, 146, Article 111417. <https://doi.org/10.1016/j.lwt.2021.111417>
- Luo, Y., Shen, M., Li, E., Xiao, Y., Wen, H., Ren, Y., & Xie, J. (2020). Effect of Mesona chinensis polysaccharide on pasting, rheological and structural properties of corn starches varying in amylose contents, 115713–115713 *Carbohydrate polymers*, 230. <https://doi.org/10.1016/j.carbpol.2019.115713>
- Ma, Y.-S., Pan, Y., Xie, Q.-T., Li, X.-M., Zhang, B., & Chen, H.-Q. (2019). Evaluation studies on effects of pectin with different concentrations on the pasting, rheological and digestibility properties of corn starch. *Food Chemistry*, 274(C), 319–323. <https://doi.org/10.1016/j.foodchem.2018.09.005>
- Malomo, S. A., & Aluko, R. E. (2015). A comparative study of the structural and functional properties of isolated hemp seed (Cannabis sativa L.) albumin and globulin fractions. *Food Hydrocolloids*, 43, 743–752. <https://doi.org/10.1016/j.foodhyd.2014.08.001>
- Malomo, S. A., Onuh, J. O., Girgih, A. T., & Aluko, R. E. (2015). Structural and antihypertensive properties of enzymatic hemp seed protein hydrolysates. *Nutrients*, 7(9), 7616–7632.
- Marinopoulou, A., Sevastopoulou, N., Farmouzi, K., Konstantinidou, E., Alexandri, A., & Papageorgiou, M. (2024). Impact of hemp (Cannabis sativa L.) protein addition on the rheological properties of wheat flour dough and bread quality. *Applied Sciences*, 14(24), 11633.
- Martinez, M. M., Li, C., Okoniewska, M., Mukherjee, I., Vellucci, D., & Hamaker, B. (2018). Slowly digestible starch in fully gelatinized material is structurally driven by molecular size and A and B1 chain lengths. *Carbohydrate polymers*, 197, 531–539. <https://doi.org/10.1016/j.carbpol.2018.06.021>
- Pang, Z., Bourouis, I., Sun, M., Cao, J., Liu, P., Sun, R., Chen, C., Li, H., & Liu, X. (2022). Physicochemical properties and microstructural behaviors of rice starch/soy protein mixtures at different proportions. *International Journal of Biological macromolecules*, 209(Pt B), 2061–2069. <https://doi.org/10.1016/j.ijbiomac.2022.04.187>
- Rawal, K., Annamalai, P. K., Ningtyas, D. W., & Prakash, S. (2024). Enhancement of emulsion stability and functional properties of hemp protein-based dairy alternative by different treatments after cellulase hydrolysis. *International Journal of Food Science and Technology*, 59(1), 639–648.
- Shao, Y., Jiao, R., Wu, Y., Xu, F., Li, Y., Jiang, Q., Zhang, L., & Mao, L. (2023). Physicochemical and functional properties of the protein–starch interaction in Chinese yam. *Food Science & Nutrition*, 11(3), 1499–1506.
- Socrates, G. (2004). *Infrared and Raman characteristic group frequencies: tables and charts*. John Wiley & Sons.
- Song, B., Xu, X., Hou, J., Liu, M., Yi, N., Zhao, C., & Liu, J. (2024). Research on corn starch and black bean protein isolate interactions during gelatinization and their effects on physicochemical properties of the blends, 127827–127827 *International Journal of Biological macromolecules*, 254(Pt 2). <https://doi.org/10.1016/j.ijbiomac.2023.127827>
- Tang, C.-H., Ten, Z., Wang, X.-S., & Yang, X.-Q. (2006). Physicochemical and functional properties of hemp (Cannabis sativa L.) protein isolate. *Journal of Agricultural and Food Chemistry*, 54(23), 8945–8950.
- Wang, C., Xue, Y., Yousaf, L., Hu, J., & Shen, Q. (2020). Effects of high hydrostatic pressure on the ordered structure including double helices and V-type single helices of rice starch. *International Journal of Biological macromolecules*, 144, 1034–1042.
- Wang, Q., & Xiong, Y. L. (2019). Processing, nutrition, and functionality of hempseed protein: A review. *Comprehensive Reviews in Food Science and Food Safety*, 18(4), 936–952. <https://doi.org/10.1111/1541-4337.12450>
- Xiao, Y., Liu, S., Shen, M., Jiang, L., Ren, Y., Luo, Y., & Xie, J. (2020). Effect of different Mesona chinensis polysaccharides on pasting, gelation, structural properties and *in vitro* digestibility of tapioca starch-Mesona chinensis polysaccharides gels. *Food Hydrocolloids*, 99, Article 105327. <https://doi.org/10.1016/j.foodhyd.2019.105327>
- Yang, C., Zhong, F., Goff, H. D., & Li, Y. (2019). Study on starch-protein interactions and their effects on physicochemical and digestible properties of the blends. *Food Chemistry*, 280, 51–58.
- Yang, H., Tang, M., Wu, W., Ding, W., Ding, B., & Wang, X. (2021). Study on inhibition effects and mechanism of wheat starch retrogradation by polyols. *Food Hydrocolloids*, 121, Article 106996. <https://doi.org/10.1016/j.foodhyd.2021.106996>
- Zhang, B., Qiao, D., Zhao, S., Lin, Q., Wang, J., & Xie, F. (2021). Starch-based food matrices containing protein: Recent understanding of morphology, structure, and properties. *Trends in Food Science & Technology*, 114, 212–231. <https://doi.org/10.1016/j.tifs.2021.05.033>
- Zhang, X., Zhou, W., Qin, X., Hou, C., & Yang, X. (2025). Preparation, Modification, Food Application, and Health Effects of Protein and Peptide from Hemp (Cannabis sativa L.) Seed: A Review of the Recent Literature. *Foods*, 14(7), 1149.
- Zheng, L., Yu, Y., Tong, Z., Zou, Q., Han, S., & Jiang, H. (2019). The characteristics of starch gels molded by 3D printing (n/a) *Journal of Food Processing and preservation*, 43(7). <https://doi.org/10.1111/jfpp.13993>
- Zhu, F., & Cui, R. (2020). Comparison of physicochemical properties of oca (Oxalis tuberosa), potato, and maize starches. *International Journal of Biological macromolecules*, 148, 601–607. <https://doi.org/10.1016/j.ijbiomac.2020.01.028>
- Zhu, P., Wang, M., Du, X., Chen, Z., Liu, C., & Zhao, H. (2020). Morphological and physicochemical properties of rice starch dry heated with whey protein isolate. *Food Hydrocolloids*, 109, Article 106091. <https://doi.org/10.1016/j.foodhyd.2020.106091>
- Zhu, Z., Wang, C., Mei, L., Xue, W., Sun, C., Wang, Y., & Du, X. (2022). Effects of soy protein isolate hydrolysate on physicochemical properties and *in vitro* digestibility of corn starch with various amylose contents. *Food Science & Technology*, 169, Article 114043. <https://doi.org/10.1016/j.lwt.2022.114043>